J Mater Sci: Mater Electron (2016) 27:3384–3389
DOI 10.1007/s10854-015-4169-7

Effect of γ-Al_2O_3 additives on the microstructure of Y_2O_3 ceramics

Zhongying Wang[1] · Le Zhang[2] · Hao Yang[2] · Jian Zhang[2] · Lixi Wang[1] · Qitu Zhang[1]

Received: 16 October 2015 / Accepted: 29 November 2015 / Published online: 12 December 2015

Abstract This paper reported the fabrication of Y_2O_3 transparent ceramics with γ-Al_2O_3 doped as the sintering aid under vacuum using the co-precipitated Y_2O_3 powders as raw materials. The different concentrations of γ-Al_2O_3 were employed for investigating the effect on the microstructures and densities of Y_2O_3 ceramics. The doped sintering aid could achieve fine microstructure and high density. The average grain sizes were around 25 μm, and the relative densities were all above 98.5 %. The best sample was achieved with 0.08 wt% γ-Al_2O_3 when sintered at 1850 °C for 8 h. And the grain size and relative density were 25 μm and 99.47 %, respectively.

1 Introduction

Y_2O_3 transparent ceramic has been investigated for many years. And the Y_2O_3 ceramic has been widely used as windows, domes, display applications and so on [1–3]. It has been proven to be an attractive candidate of the laser materials due to its high thermal conductivity, broad range of transparency, stable physical and chemical properties, strong stark-splitting and relatively low phonon energies [4]. However, owing to the high melting point at 2410 °C, the development of Y_2O_3 transparent ceramics was hindered [5]. So far, many methods were employed to fabricate Y_2O_3 powders. Such as sol–gel method [6, 7], electrospray pyrolysis [8], hydrothermal synthesis [9], chemical coprecipitation [10], etc. Meanwhile, the chemical precipitation has a relative superiority for preparation of excellent powders, which is beneficial for sintering and could be expanded to mass production.

For chemical precipitation, ammonia water or ammonium hydrogen carbonate was usually selected as precipitant [11, 12]. When the ammonia water and ammonium hydrogen carbonate are all used as mixed precipitant, the appropriate ratio of them could be employed to obtain excellent precursors [13]. Appropriate sintering aids are pivotal factors for high grade transparent ceramics [14]. In the previous research, ZrO_2 and La_2O_3 were selected as the sintering aids. However, too much sintering aids are not beneficial for the laser and strength properties of transparent ceramics [15–17]. By using ZrO_2 as the sintering aid, the Y_2O_3 ceramics with small grain size were successfully achieved [18]. However, the high sintering temperature and longtime duration were also required. Moreover, La_2O_3 as the sintering aid could reduce sintering temperature of high transparent Y_2O_3 ceramic. However, the crystalline grain abnormally grown up and the size was distributed in a wide range [19]. The γ-Al_2O_3 used as the sintering aids was little reported, and the effect of Al_2O_3 on the microstructure has also few reported.

In this research, the γ-Al_2O_3 was used as sintering aid. The effect of different concentrations of γ-Al_2O_3 on the microstructure was studied. The relationship of the volume shrinkage and density of the Y_2O_3 ceramics was also investigated.

✉ Jian Zhang
jzhang@jsnu.edu.cn

✉ Qitu Zhang
ngdzqt@163.com

[1] College of Materials Science and Engineering, Nanjing Tech University, Nanjing 210009, China

[2] Jiangsu Key Laboratory of Advanced Laser Materials and Devices, School of Physics and Electronic Engineering, Jiangsu Normal University, Xuzhou 221116, China

2 Experiment

0.20 mol/L $Y(NO_3)_3$ solution was used as a mother solution. And a 1.5 mol/L ammonium hydrogen carbonate and a 2 mol/L ammonium hydroxide were used as the mixed precipitant solution. The mother solution (4 L) was stirred at 320 rpm. Then, the precipitant solution was dripped into the mother solution at a rate of 5 ml/min. The final pH value of the slurry was 8.0. Meanwhile, 10.57 g ammonium sulfate as dispersant was added into the slurry with stirring for a half hour. The precipitations were aged for 36 h at the room temperature. Then they were filtered and washed with three times using the deionized water and anhydrous ethanol severally. The aim was to completely remove byproducts of the precipitation reaction, such as NH^{4+} and NO^{3-} [20].

After filtered, the precipitate was dried at 60 °C for 24 h in infrared drying oven. And the dried precipitate would be crushed and refined by the 100 mesh sieve. Then precursors were calcined at 1300 °C for 3 h in the furnace. The obtained Y_2O_3 powders and a small amount of γ-Al_2O_3 were ball-milled with alumina balls for 12 h at 140 rpm, and the weight ratio of ball: powder: alcohol is 6:1:2, the diameter of the balls is 3.0 mm (small). 0, 0.04, 0.08, 0.12, 0.16 and 0.20 wt% γ-Al_2O_3 were added in the Y_2O_3 powders with ethanol, respectively. The slurry was dried at 55 °C for 24 h. Then dried slurry was sieved through 100 mesh. After removing organic components by calcined at 850 °C for 5 h, the powders were dry pressed into Φ15 mm disk in a stainless steel mould at 25 MPa. The green bodies were further cold isostatically pressed (CIPed) at 200 MPa for 5 min. All disks were sintered at 1850 °C for 8 h with a rate of 1 °C/min in the vacuum sintering furnace utilizing a tungsten heating elements under a vacuum of 10^{-4} Pa. Then sintered ceramics were annealed at 1400 °C for 10 h and mirror polished at 2 mm thickness.

Thermo-gravimetric and differential scanning calorimetry (TG-DSC, EXSTAR DSC6000, Hitachi, Japan) was used to analyzed the physiochemistry process in the calcined precursor. Phase identification was performed by an X-ray powder diffraction (XRD, D2 PHASER, Bruker, Germany) pattern analysis. The morphologies of the precursors before and after calcination were observed by using a Field emission scanning electron microscopy (FESEM, S4800, Hitachi, Japan). The relative densities of all sintered ceramics were measured by the Archimedes method with the theoretical density of Y_2O_3 as 5.031 g/cm^3. Scanning electron microscopy (SEM, JSM-6510LV, JEOL, Japan) was used to observe the microstructure of the thermal etched surfaces and the fracture surfaces of Y_2O_3 ceramic. The thermal expansion coefficients of Y_2O_3 ceramics were obtained by using a thermal mechanical analyzer (TMA, DIL402E, Netzsch, Germany).

3 Results and discussion

Figure 1 is TG/DSC analysis curve of the precursor. There are three general decomposition processes in the curve. The first stage is under 200 °C, the endothermic peak at 134 °C was attributed to the removal of absorbed and molecular water. The second stage is a main mass-loss process, and about 45 % mass loss occurred between 200 and 800 °C. An exothermic peak at 550 °C was attributed to the decomposition of yttrium carbonate, yttrium hydroxide and the crystal water. The exothermic peak at 703 °C indicated the crystallization of yttria. And the third stage is behind 800 °C. A broad endothermic peak centered at 1155 °C was ascribed to the decomposition of SO_4^{2-}. The SO_4^{2-} can be absorbed onto the surface of the precursor particles due to the electro-static force. It has a higher decomposition temperature than the precursor and its existence at comparatively high temperature may reduce the element diffusion between particles, resulting in a smaller particle size [21].

Figure 2 shows the XRD patterns of the synthesized precursors and calcined powders. As shown in Fig. 2a, three peaks were observed, which indicated that the component of precursor were $Y(NO_3)_3{\cdot}6H_2O$, $Y_2(CO_3)_3{\cdot}2H_2O$ and small amount of $Y(OH)_3$. As shown in Fig. 2b, the precursors with different concentrations of γ-Al_2O_3 were calcined at 1300 °C. Pure Y_2O_3 crystalline phase was obtained and no other crystalline phase was detected. The average crystalline size of calcined powders was calculated from Scherrer's formula. The crystalline size of Y_2O_3 powders with 0, 0.04, 0.08, 0.12, 0.16 and 0.20 wt% γ-Al_2O_3 is 59.3, 59.7, 60.3, 59.8, 61.1 and 60.7 nm, respectively. Therefore, the addition of γ-Al_2O_3 had a little effect on the crystalline size.

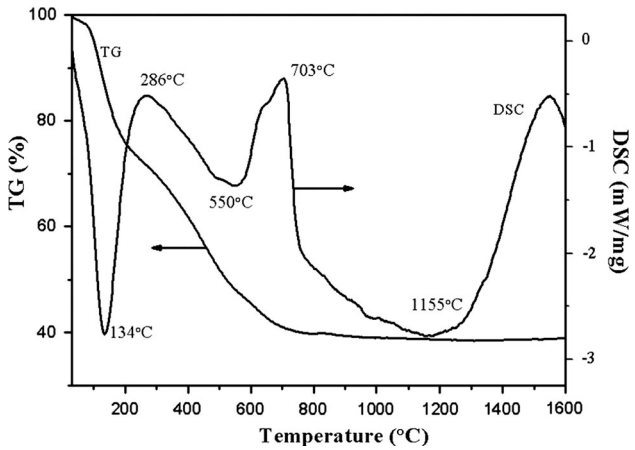

Fig. 1 TG/DSC curves of the precursor

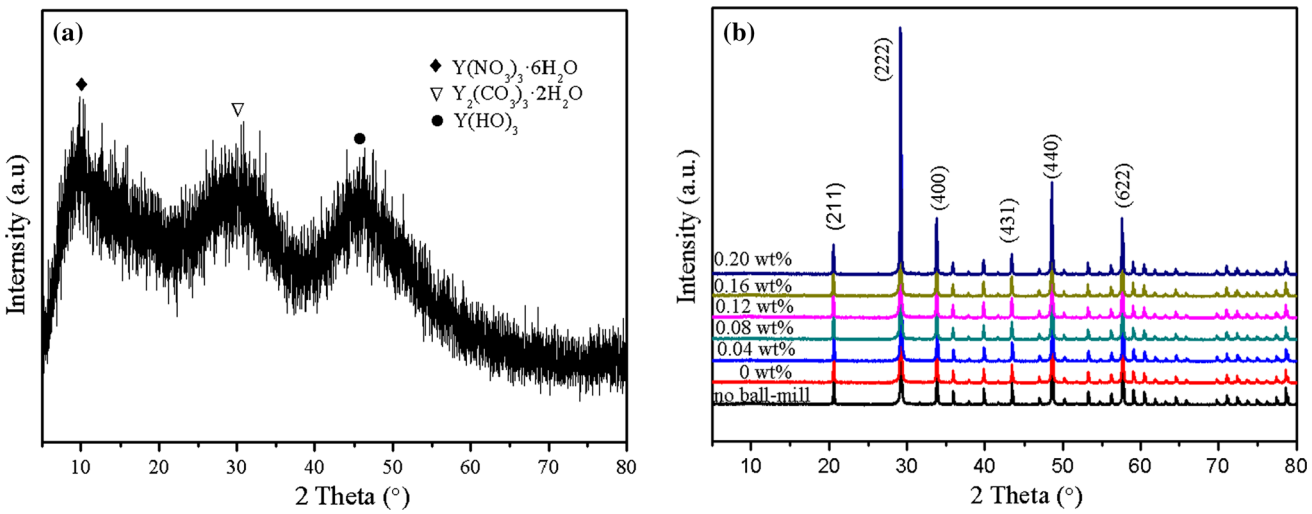

Fig. 2 XRD patterns of **a** the precursors and **b** Y_2O_3 powders with different concentrations of γ-Al_2O_3 and no ball-milled

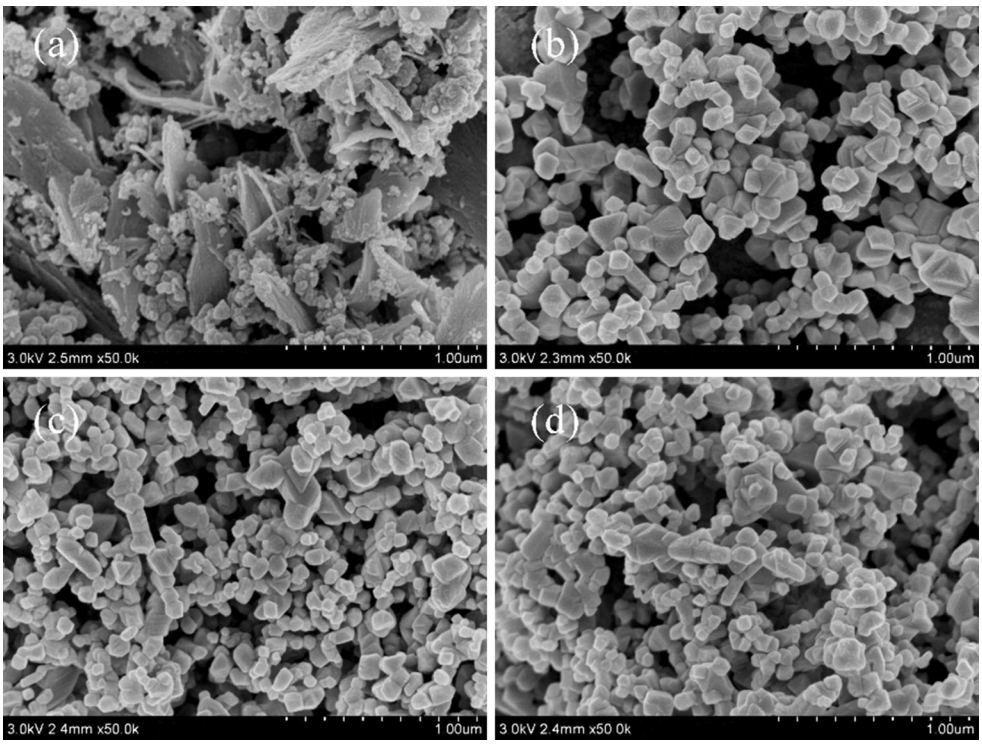

Fig. 3 FESEM morphology of **a** the precursors, Y_2O_3 powders **b** with no ball-milling and with the concentrations of **c** 0.08 wt% and **d** 0.12 wt% γ-Al_2O_3 calcined at 1300 °C

Figure 3 is the FESEM images of the precursors and the Y_2O_3 powders. As shown in Fig. 3a, the precursors were composed of the granular $Y_2(CO_3)_3 \cdot 2H_2O$ and the sheet $Y(OH)_3$. The activity of $Y_2(CO_3)_3 \cdot 2H_2O$ was better than that of $Y(OH)_3$ in the theory. And the size of $Y_2(CO_3)_3 \cdot 2H_2O$ was about 10 nm, most of the granular $Y_2(CO_3)_3 \cdot 2H_2O$ were agglomerated that dispersed on the sheet $Y(OH)_3$, and the sheet $Y(OH)_3$ was quite a few in the precursors, but $Y(NO_3)_3 \cdot 6H_2O$ could not be found nearly from the appearance. Figure 3b shows the FESEM image of no ball-milled Y_2O_3 powders without γ-Al_2O_3, in which little agglomeration was visible. And as shown in Fig. 3c, d, no obvious sintering necks could be found. In addition, the shape and size of all Y_2O_3 powders were similar. Therefore, the concentration of γ-Al_2O_3 had little apparent effect on the shape of powders. Higher calcined temperature might lead to a bigger powder size with lower sintering activity.

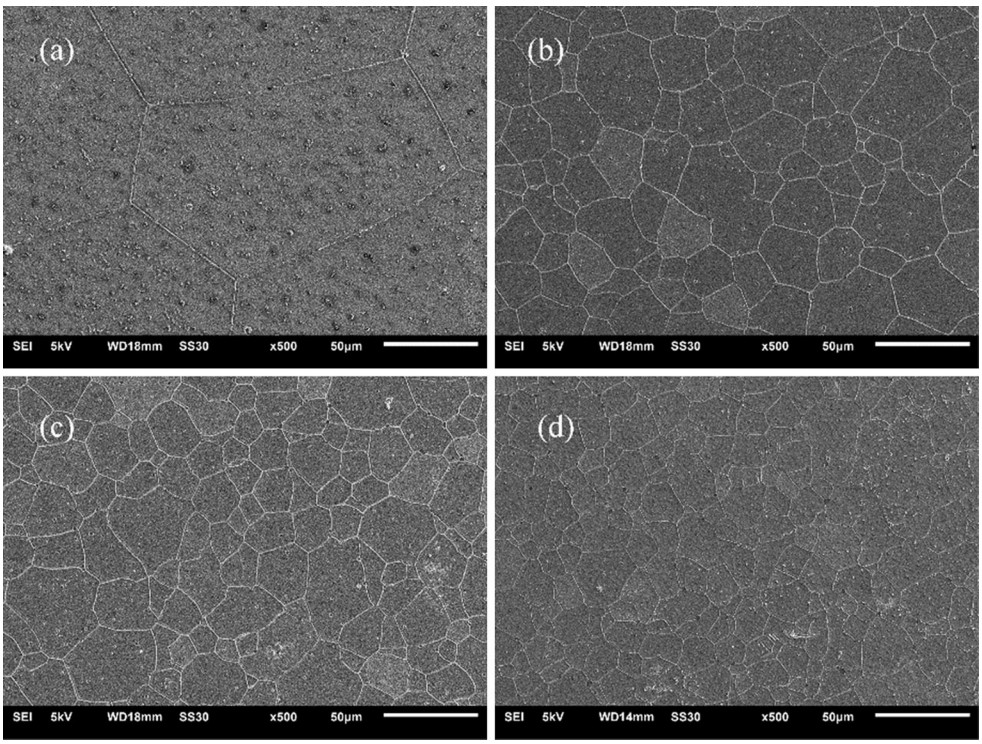

Fig. 4 SEM images of thermal etched surfaces of Y_2O_3 ceramics with **a** no ball-milled, **b** 0.04 wt%, **c** 0.08 wt% and **d** 0.20 wt% γ-Al_2O_3

Figure 4 shows the SEM images of the thermal etched surfaces of Y_2O_3 ceramics, which were sintered at 1850 °C for 8 h and annealed at 1400 °C for 10 h. In Fig. 4a, the grain size of the sample without γ-Al_2O_3 was about 150 μm. As shown in Fig. 4b, when the concentration of γ-Al_2O_3 was 0.04 wt %, the size of the Y_2O_3 ceramics crystalline grain was about 40 μm that was resulted by γ-Al_2O_3 through the process of ball-milling, which indicated the just a little γ-Al_2O_3 had the effect of restraining the growth of crystalline grain. As shown in Fig. 4c, the grain size of the sample with 0.08 wt% γ-Al_2O_3 was about 25 μm. As shown in Fig. 4d, when the concentration of γ-Al_2O_3 was 0.20 wt%, the grain size was about 20 μm. Obviously, the grain sizes were smaller with the concentration of γ-Al_2O_3 increasing.

It is clearly that a small amount of γ-Al_2O_3 could refine the grain size of Y_2O_3 ceramics. However, when the concentrations of γ-Al_2O_3 were higher, the grain size was not clearly change smaller. And the average grain size was all about 20–40 μm. In this study, the γ-Al_2O_3 could restrain the grain-boundary mobility, and then inhibits the faster grain growth. Moreover, the smaller grain size was beneficial for the densification and strength of Y_2O_3 ceramics [17].

Figure 5 indicates the SEM images of the fracture surfaces of Y_2O_3 ceramics with different concentration of γ-Al_2O_3. About 100–200 μm grains could be found without ball-milling. And the grain size was about 40 μm when the concentration of γ-Al_2O_3 was 0.04 wt%. With the concentration of γ-Al_2O_3 up to 0.08 wt%, the grain size was reduced to 20 μm. It is clearly that γ-Al_2O_3 could decrease the grain size with fine microstructure. With the increase of γ-Al_2O_3 to 0.20 wt%, the grain size decreased to 15 μm. The grain sizes changed slowly when the concentrations of γ-Al_2O_3 were more than 0.08 wt%.

The Fig. 6 shows the linear shrinkage and linear shrinkage rate of the Y_2O_3 samples with 0 and 0.08 wt% γ-Al_2O_3 through TMA. The sample with 0 wt% γ-Al_2O_3 was shrinkable beginning at about 1000 °C, and the apparent shrinkage was at 1510 °C. For the sample with 0.08 wt% γ-Al_2O_3, the beginning shrinkage temperature was about 1200 °C, and the shrinkage rate reached highest at 1490 °C. The peak of the shrinkage rate of Y_2O_3 sample with 0.08 wt% γ-Al_2O_3 was broader and lower than the sample with 0 wt% γ-Al_2O_3. The γ-Al_2O_3 could restrain the faster grain growth that was beneficial for fine grain growth, reducing wrapped pores and eliminating pores to enhance properties of sample sintering process. So the sample with 0.08 wt% γ-Al_2O_3 should have a smaller grain size, which was consistent with the TMA analysis that conformed to previous conclusions.

In this study, the grain size of Y_2O_3 ceramics became smaller when the γ-Al_2O_3 was used as sintering aid. As shown in the Fig. 7, the Y_2O_3 ceramics obtained smallest

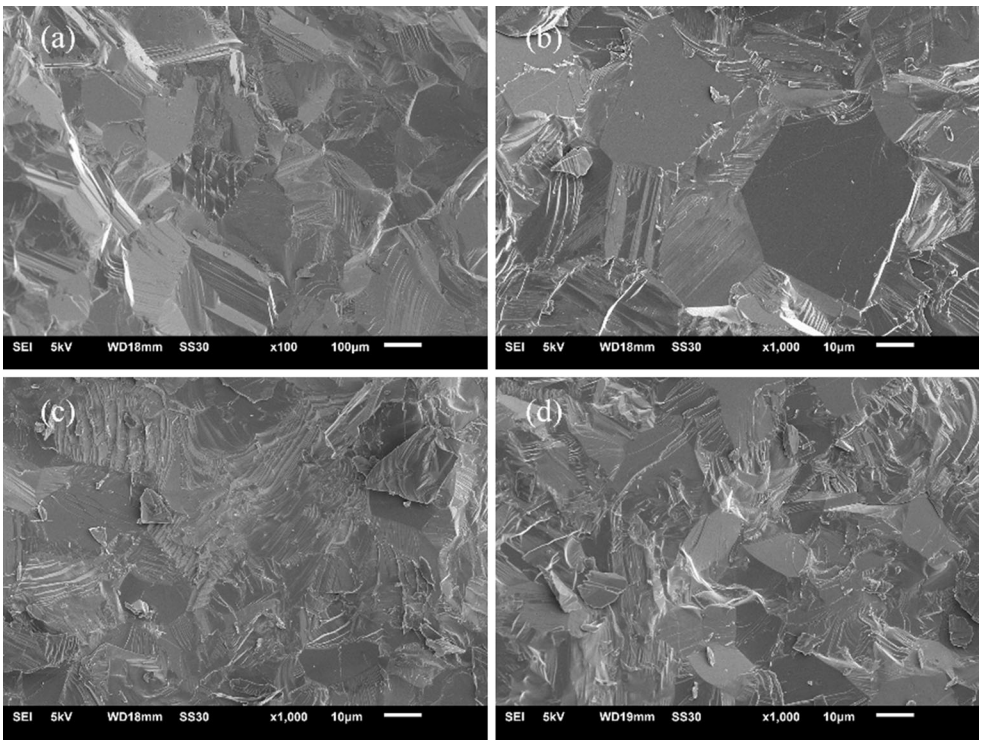

Fig. 5 SEM images of fracture surfaces of Y_2O_3 ceramics with **a** no ball-milled, **b** 0.04 wt%, **c** 0.08 wt% and **d** 0.20 wt% γ-Al_2O_3

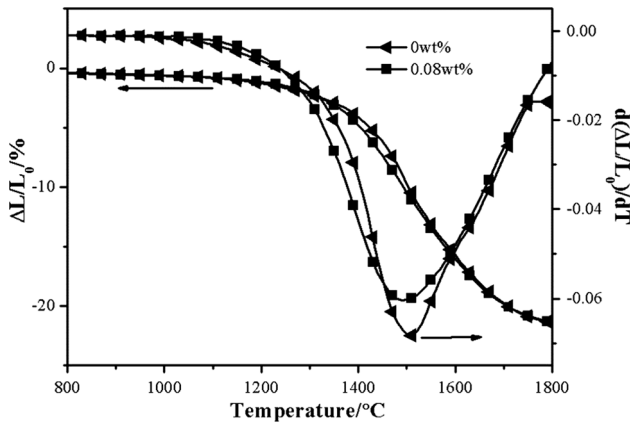

Fig. 6 Thermal mechanical analyzer thermogram of Y_2O_3 samples with the concentration 0 and 0.08 wt% γ-Al_2O_3

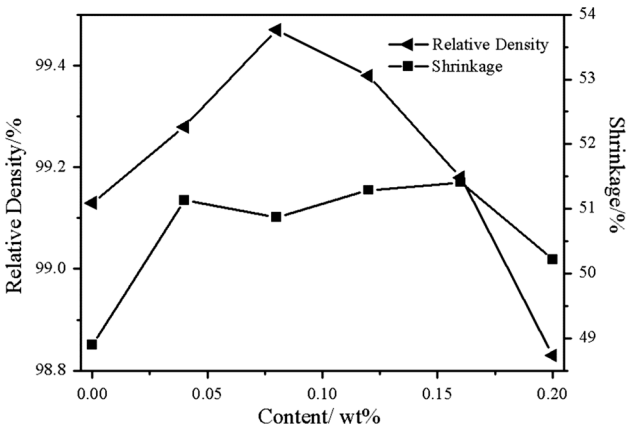

Fig. 7 The densities and volume shrinkages of Y_2O_3 ceramics with different concentrations of γ-Al_2O_3

grain size was at the concentration of 0.08 wt% γ-Al_2O_3. The relative density of samples was 99.47 % that was higher than that of others. The relative density of most samples was over 99 %, and it proved the most samples were compact that was beneficial for the strength of Y_2O_3 ceramics. And the volume shrinkage of 0.04–0.16 wt% γ-Al_2O_3 was similar at about 51 % after sintering. When the concentration of γ-Al_2O_3 was added to 0.20 wt%, the volume shrinkage was less among them. Therefore, in the term of density and shrinkage, the concentration of 0.08 wt% γ-Al_2O_3 was the best. The smaller of grain sizes of the different doping concentrations, the higher mechanical and optical properties [22]. And at the same experimental conditions, the mechanical property of the Y_2O_3 transparent ceramics was higher with the smaller grain size [23]. And the grain size of the no-doped Y_2O_3 ceramics was larger about 150 μm, but the grain sizes of others with the concentrations of the γ-Al_2O_3 were smaller. When the concentration of γ-Al_2O_3 was 0.08 wt%, the grain size was about 25 μm, and the density and volume shrinkage of Y_2O_3 ceramics with the concentration of 0.08 wt% γ-Al_2O_3 were higher.

4 Conclusions

This paper investigate the influence of γ-Al_2O_3 as sintering aid on the microstructure and the relative densities of Y_2O_3 ceramics. The sample with 0.08 wt% γ-Al_2O_3 could be achieved fine microstructure and highest relative density at 1850 °C for 8 h under vacuum. The average grain size was around 25 μm, and the relative density of Y_2O_3 ceramic was 99.47 %. The γ-Al_2O_3 could restrain the faster grain growth that was beneficial for the process of eliminating pores and reducing wrapped pores at sintering process to enhance properties of Y_2O_3 ceramics. Through the further research, better optical transparency of Y_2O_3 ceramics can be secured by the appropriate additive amount of γ-Al_2O_3 as the sintering aid. And highly transparent Y_2O_3 ceramic as a promising material would be mainly applied in medical CT, laser gain medium and windows.

Acknowledgments The authors acknowledge the generous financial support from Priority Academic Program Development of Jiangsu Higher Education Institutions (PAPD), and National Natural Science Foundation of China (51402133, 51302115, and 51202111).

References

1. H. Eilers, J. Eur. Ceram. Soc. **27**(16), 4711 (2007)
2. J.R. Lu, J.H. Lu, T. Murai, K. Takaichi, T. Uematsu, K. Ueda, H. Yagi, T. Yanagitani, A.A. Kaminskii, Jpn. J. Appl. Phys. **40**(12A), 1277 (2001)
3. C. Greskovich, S. Duclos, Annu. Rev. Mater. Sci. **27**, 69 (1997)
4. J. Zhang, L. An, M. Liu, S. Shimai, S. Wang, J. Eur. Ceram. Soc. **29**(2), 305 (2008)
5. J.R. Lu, K. Takaichi, T. Uematsu, A. Shirakawa, M. Musha, K. Ueda, H. Yagi, T. Yanagitani, A.A. Kaminskii, Jpn. J. Appl. Phys. **41**(12A), 1373 (2002)
6. J. Wang, D. Chen, E.H. Jordan, M. Gell, J. Am. Ceram. Soc. **93**(11), 3535 (2010)
7. M. Wang, R. Zuo, S. Qi, L. Liu, J. Mater. Sci.: Mater. Electron. **23**(3), 753 (2012)
8. A.J. Rulison, R.C. Flagan, J. Am. Ceram. Soc. **77**(12), 3244 (1994)
9. P.K. Sharma, M.H. Jilavi, R. Nar, H. Schmidt, J. Mater. Sci. Lett. **17**(10), 823 (1998)
10. Z. Huang, W. Guo, B.J. Fei, J.T. Li, Y.G. Cao, Mater. Res. Innov. **17**(2), 73 (2013)
11. Y. Liu, X. Qin, H. Xin, C. Song, J. Eur. Ceram. Soc. **33**(13–14), 2625 (2013)
12. W.J. Li, H. Lin, H. Teng, N. Liu, Y.K. Li, X.R. Hou, T.T. Jia, S.M. Zhou, Chin. J. Inorg. Chem. **26**(4), 687 (2010)
13. Y. Shi, J.Y. Chen, J.L. Shi, Mater. Sci. Forum **492–493**, 101 (2005)
14. H.J. Wu, T.C. Lu, N. Wei, Z.W. Lu, X.T. Chen, Y.B. Guan, Y. Zhao, J.Q. Qi, Q.W. Shi, X.M. Xie, W. Zhang, J. Mater. Sci.: Mater. Electron. **26**(4), 2451 (2015)
15. Q. Yi, S. Zhou, H. Teng, H. Lin, X. Hou, T. Jia, J. Eur. Ceram. Soc. **32**(2), 381 (2012)
16. Q. Lu, Q. Yang, C. Jiang, S. Lu, Y. Yuan, Q. Liu, B. Lu, Opt. Mater. **37**, 115 (2014)
17. X. Hou, S. Zhou, T. Jia, H. Lin, H. Teng, J. Eur. Ceram. Soc. **5**(5), 733 (2011)
18. X. Hou, S. Zhou, W. Li, Y. Li, J. Eur. Ceram. Soc. **30**(15), 3125 (2010)
19. B.K. Jang, S. Kim, Y.S. Oh, H.T. Kim, Y. Sakka, H. Murakami, J. Ceram. Soc. Jpn. **119**(1396), 929 (2011)
20. C. Marlot, E. Barraud, S. Le Gallet, M. Eichhorn, F. Bernard, J. Solid State Chem. **191**(7), 114 (2012)
21. N. Wang, X. Zhang, G. Qiu, H. Sun, Q. Liu, X. Mi, X. Wang, J. Rare Earths **28**(2), 232 (2010)
22. J.M. Luo, Z.C. Zhong, J.L. Xu, Mater. Res. Bull. **47**(12), 4283 (2012)
23. O. Yeheskel, I.C. Albayrak, B. Anasori, M.W. Barsoum, J. Eur. Ceram. Soc. **31**(9), 1703 (2011)